

# **Modelling of a thin-walled filament-wound composite cylinder using an axisymmetric approach**

Tom Thorvaldsen and Harald Osnes

Norwegian Defence Research Establishment (FFI)

30 March 2011

FFI-rapport 2011/00735

371701

P: ISBN 978-82-464-1903-9

E: ISBN 978-82-464-1904-6

## Keywords

Kompositt

Tynnvegget sylinder

Trykktank

Aksesymmetrisk modell

MSC.Marc/Mentat

## Approved by

Einar Willassen

Project Manager

Jan Ivar Botnan

Director

## English summary

In this report, finite element analyses (FEA) are performed for a thin-walled filament-wound composite cylinder exposed to an inner pressure load. Analyses are run for an open cylinder, as well as for a closed cylinder. The purpose of the study is to gain enhanced knowledge on how to model cylindrical structures using an axisymmetric model approach. The commercial software package MSC.Marc/Mentat 2008r1 is employed in the analyses.

Both continuum and composite axisymmetric elements are included in the FEA. In addition, different methods are applied for calculating the element stiffness properties. The choice of element type and definition of the element stiffness properties will influence on the properties of each physical layer of the structure, as well as the overall response of the structure. The FEA results are compared both with analytical calculations and Laminated Tube.

The axisymmetric continuum element is found to be applicable for modelling the cylindrical composite structure; the FEA results are in good agreement with analytical calculations, as well as the results obtained using Laminated Tube. However, the FEA results when employing axisymmetric composite elements in the modelling are not in accordance with either the analytical calculations or Laminated Tube. Hence, the composite element type investigated does not seem to be applicable for this type of analysis.

## Sammendrag

Denne rapporten beskriver elementmetodeanalysene som er gjort for en tynnvegget, viklet sylinder i kompositt, utsatt for en indre trykklast. Analyser er utført både for en åpen sylinder og en lukket sylinder. Målet med studien er å få bedre forståelse av og kunnskap om hvordan man skal modellere sylindriske konstruksjoner ved å bruke en aksesymmetrisk modelltilnærming. Den kommersielle programvarepakken MSC.Marc/Mentat 2008r1 er benyttet i analysene.

Både aksesymmetriske kontinuumelementer og komposittlementer er benyttet i analysene. I tillegg er det brukt ulike metoder for å beregne stivhetsegenskapene til elementene. Valg av elementtype og definisjon av elementets stivhetsegenskaper vil påvirke egenskapene til hvert av de fysiske lagene i konstruksjonen, så vel som egenskapene til konstruksjonen som helhet. Elementmetodeanalysene er sammenliknet med både analytiske beregninger og Laminated Tube.

Det aksesymmetriske kontinuumelementet egner seg for modellering av den sylindriske konstruksjonen i kompositt; elementmetodeanalyseresultatene er i god overensstemmelse med analytiske beregninger, så vel som resultatene fra Laminated Tube. Resultatene fra analysene der komposittlementer er benyttet, er derimot ikke i overensstemmelse med verken analytiske beregninger eller Laminated Tube. Det aksesymmetriske komposittlementet virker derfor ikke å være egnet for denne typen analyser.

## Contents

<b>1</b>	<b>Introduction</b>	<b>7</b>
<b>2</b>	<b>Case study</b>	<b>7</b>
<b>3</b>	<b>FEM model in MSC.Marc</b>	<b>9</b>
3.1	Geometry	9
3.2	Element type and lay-up	10
3.2.1	Continuum elements	10
3.2.2	Composite elements	10
3.3	Material properties and stiffness relations	11
3.3.1	Continuum elements	11
3.3.2	Composite elements	12
3.4	Boundary conditions	14
3.5	Applied loads	15
3.5.1	Open cylinder	15
3.5.2	Closed cylinder	15
<b>4</b>	<b>Analytical method</b>	<b>16</b>
<b>5</b>	<b>Laminated Tube</b>	<b>18</b>
<b>6</b>	<b>Test cases</b>	<b>19</b>
6.1	Case #1: [45/90/45/90]	19
6.1.1	Continuum elements	20
6.1.2	Composite elements	22
6.1.3	Discussion	24
6.2	Case #2: [0/90/0/90]	26
6.2.1	Continuum elements – open cylinder	26
6.2.2	Continuum elements – closed cylinder	27
6.2.3	Composite elements – open cylinder	27
6.2.4	Composite elements – closed cylinder	27
6.2.5	Discussion	28
6.3	Case #3: [10/90/30/90]	28
6.3.1	Continuum elements	29
6.3.2	Composite elements	31
6.3.3	Discussion	32
<b>7</b>	<b>Summary and conclusions</b>	<b>33</b>

<b>Acknowledgements</b>	<b>34</b>
<b>Appendix A Material data</b>	<b>35</b>
<b>Appendix B Analytical model</b>	<b>36</b>
<b>Appendix C Mentat input files</b>	<b>43</b>
<b>References</b>	<b>44</b>

## 1 Introduction

Performing finite element analyses (FEA) of a filament-wound composite structure is a challenging task. The model should represent the properties of the physical structure as correct and precise as possible. However, when employing the finite element method (FEM), some assumptions and approximations have to be made. One important part of the modelling that often must be taken into account is the thickness variation and the fibre angle variation for each layer, which is relevant for complex geometries, in particular. Moreover, the number of elements required for each physical layer, the element stiffness calculation for each element, and the overall representation of the material properties of the composite structure, should be considered. The most physically representative approach may not give accurate numerical results. Furthermore, the boundary conditions should be carefully set – especially when utilizing symmetry properties to reduce the complexity and overall size of the geometric model. Finally, the modelling of the applied loads, the choice of element type, and the solution method are all important parts of the analysis that will have influence on the final result.

Previous modelling of filament-wound composite structures performed at FFI, such as four-inch pressure vessels and rocket motor cases, has considered an axisymmetric model. However, the results obtained from the FEA are not always in accordance with Laminated Tube, which is an Excel-based modelling tool, developed at FFI in a former project, for calculating the in-plane stresses in layered cylindrical structures. Laminated Tube is often employed in the early development phase, for a quick calculation of the lay-up required to withstand the inner pressure load and other forces acting on the structure. This study has been conducted to obtain a thorough understanding of why the results differ. The outcome of the study is twofold: 1) to verify that Laminated Tube calculates correct stress values, and 2) to obtain a better understanding of how to model filament-wound composite pressure vessels and rocket motor structures using an axisymmetric finite element model approach.

A set of test cases for a thin-walled composite cylinder structure is run using the commercial software package MSC.Marc/Mentat 2008r1. The element stiffness calculation approach and the element type is varied for each test case. The numerical results for both an open and a closed cylinder are compared with analytical calculation results, as well as with results from Laminated Tube. By choosing a thin-walled cylinder, i.e. a composite cylinder where the total wall thickness is small compared to the radius of the cylinder, analytical expressions are available.

The results from this study will be very important for future modelling of filament-wound structures.

## 2 Case study

As indicated in the introduction, the model problem chosen is a thin-walled (hollow) filament-wound composite cylinder, as shown in Figure 2.1. The inner radius is 200 mm, and the wall thickness is 2 mm. In this way, the thickness-to-radius ratio is very small, and hence analytical

expressions are available for comparison with the finite element model results. The length of the cylindrical tube is 20 mm.

Four physical layers are defined through the thickness of the cylinder, as indicated in Figure 2.1. The thickness of each physical layer is 0.5 mm. Moreover, different fibre orientations are assumed for the layers, indicated by different colours in the figure.

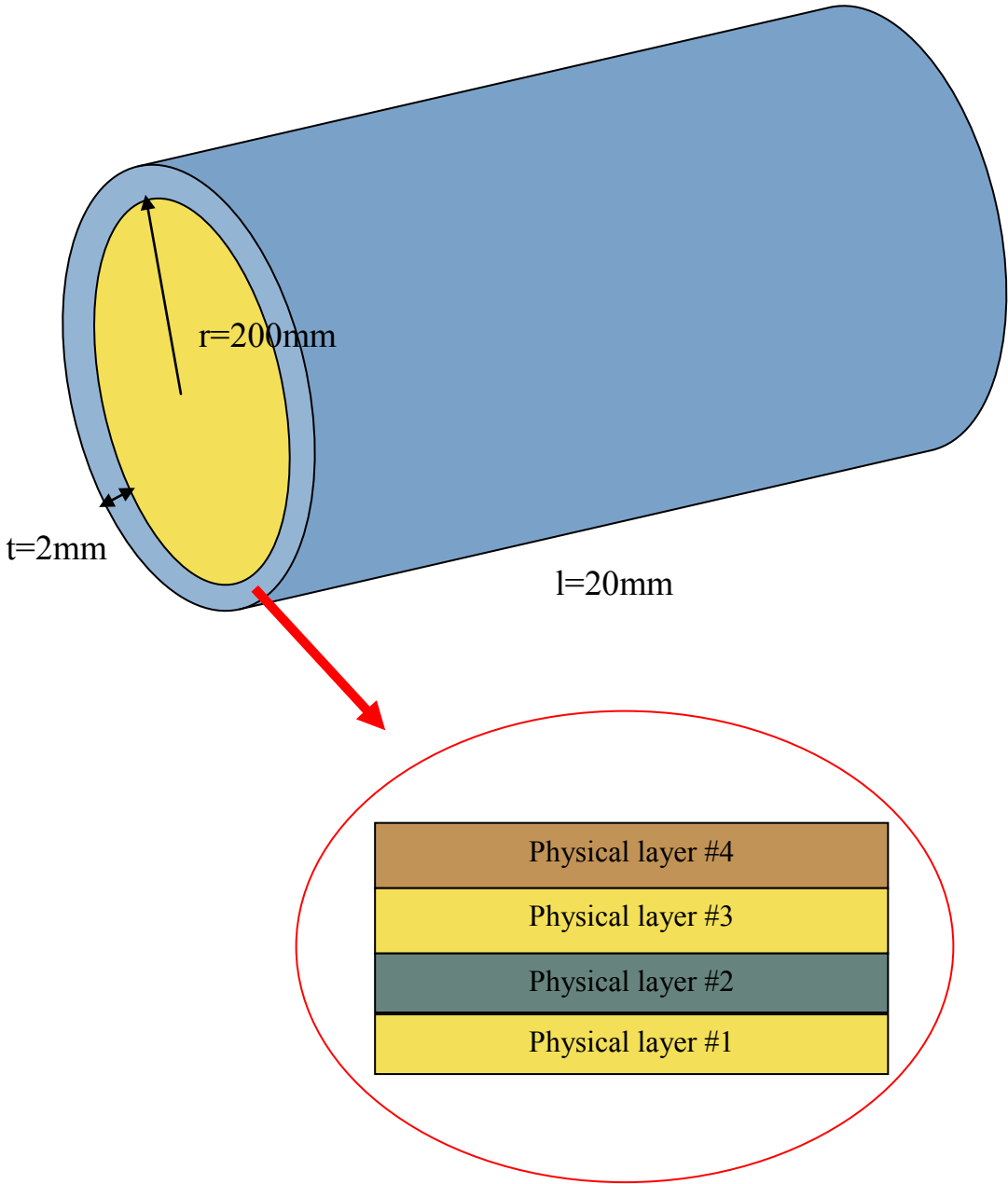


Figure 2.1 Geometric model of a thin-walled filament-wound composite cylinder with four physical layers. Different colours indicate layers with different fibre orientation.



Three test cases, i.e. three different lay-ups, are included in this study. These cases are considered as relevant and representative for comparison of the different modelling approaches:

- Case #1: [ $\pm 45 / 90 / \pm 45 / 90$ ]
- Case #2: [ $0 / 90 / 0 / 90$ ]
- Case #3: [ $\pm 10 / 90 / \pm 30 / 90$ ]

More details and the modelling results are found in Section 6.

### 3 FEM model in MSC.Marc

As described above, a thin-walled composite cylinder is our model problem. This geometry is relatively simple, but it is still relevant as a reference for more complex finite element geometries. One of the main advantages is that we can compare the FEA results with analytical expressions and Laminated Tube.

The different parts of the FEA are described in the following.

#### 3.1 Geometry

The geometric finite element model applied is shown in Figure 3.1. The axisymmetric cylinder model has a length  $l = 10$  mm and an inner radius  $r = 200$  mm. Only half of the cylinder is included in the model due to symmetry; boundary conditions at the artificial symmetry cut-plane are specified in Section 3.4.

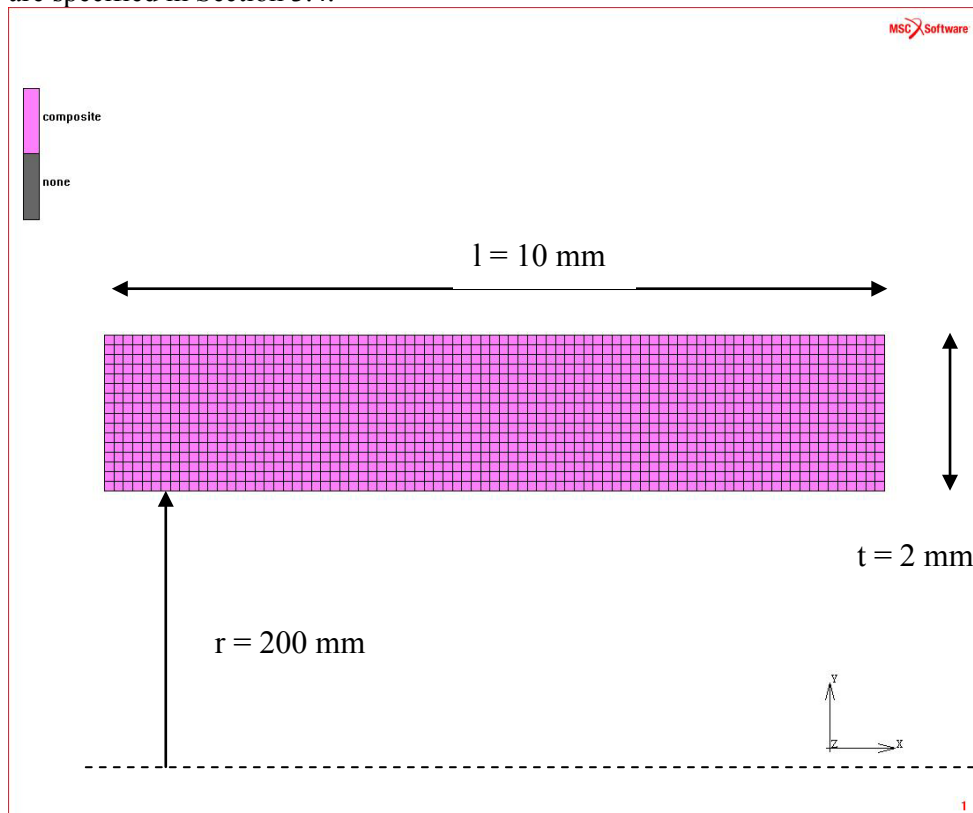


Figure 3.1 Geometry of the axisymmetric model.

## 3.2 Element type and lay-up

In all cases, four *physical layers* with different fibre orientations are defined. The fibre orientation of the four physical layers of the structure, i.e. the lay-up, is shown for each of the three test cases in Section 6. For all test cases included, the lay-up is a combination of *helical* layers and *hoop* layers. The helical layers make an angle  $0 \leq \theta < 90^\circ$  with the global axial axis, whereas the hoop layers are oriented in the circumferential direction, i.e. perpendicular to the axial axis. For example, in the first test case (Section 6.1) the lay-up is defined by  $[\pm 45 / 90 / \pm 45 / 90]$ , that is, the first and the third layers are helical layers, whereas the second and fourth layers are hoop layers.

As can be seen from Figure 3.1, a total of sixteen elements, in the thickness direction, are included in the model, which means that each physical layer is modelled by four elements (in the thickness direction). In this study, one of the key themes is the modelling of the stiffness properties of each physical layer. Hence, different lay-ups on element level for the physical layers are applied.

More details about the calculation of the stiffness properties in each of the modelling approaches are included in Section 3.3. We also refer to the MSC.Marc/Mentat documentation [1] for more details about the element types than provided in the following.

### 3.2.1 Continuum elements

For the continuum element cases, MSC.Marc element type 20 is employed, which is a four-node, isoparametric, arbitrary quadrilateral element for axisymmetric applications, including torsional strains.

Two different approaches for calculating the element stiffness properties are considered. For the case where merged stiffness values are applied, all elements in a single physical layer are given the same material properties. For the cases where non-merged stiffness values are applied, the material properties may vary for the elements within a physical layer.

### 3.2.2 Composite elements

For the composite element cases, MSC.Marc element type 152 is employed, which is a four-node, isoparametric composite element for axisymmetric applications. It is possible to define up to 1020 internal layers within the element, and the different layers can have different material properties.

Two different element material properties approaches are employed. For the case where merged stiffness properties are applied, the internal composite element layer properties vary through the element thickness, but all elements making up the physical layer are given the same properties. For the case where non-merged values are used, the internal composite element layer properties are the same through the element thickness, but in this case the elements making up the physical layer are given different properties.

### 3.3 Material properties and stiffness relations

The material data for all test cases are given in Table A1. The material parameter values refer to the fibre axes, where the first axis is directed along the fibre, and the other two axes are oriented normal to the fibre direction defined by the right-hand rule. For the continuum element cases, an anisotropic material description is applied, while an orthotropic material description is used for the composite element cases.

#### 3.3.1 Continuum elements

For the test cases where continuum elements are employed, a transformation operator is applied for expressing the stiffness matrix and the stress vector referred to local element axes, which in the software are referred to as the *preferred axes*. The stiffness matrix, referred to preferred axes, is in each case given as input to Mentat. The transformation operator applied, is described in [2]. Note that another orientation of the coordinate systems is chosen in this report compared to what was employed in the cited report; this will have influence on the declaration of the angles between the axes in the two coordinate systems.

##### 3.3.1.1 Orientation

The preferred axes for the continuum element  $(x, y, z)$  are defined as shown in Figure 3.2. Using the ORIENTATIONS functionality, the direction of the first axis is set. From this, the second axis is (automatically) defined normal to the first axis in the element plane. The direction of the third axis is found from calculating the cross-product of the first and second axes, applying the right-hand rule.

The relationship between the fibre axes  $(f, s, n)$  and the preferred axes for the continuum element is also displayed in Figure 3.2. The fibre axis  $(f)$  is rotated an angle  $\theta$  about the second preferred axis  $(y)$ , which is identical to the third axis  $(n)$  of the fibre coordinate system.

Note that the positive fibre orientation angle for the continuum elements corresponds to a negative fibre orientation angle for the composite elements, see Section 3.3.2.1. This is taken into account when defining the material properties and comparing the different approaches in the test cases presented.

##### 3.3.1.2 Stiffness calculation

Two different approaches are applied in defining the element stiffness properties:

- Merged stiffness values
- Non-merged stiffness values

In case of using *merged stiffness values*, the  $6 \times 6$  stiffness matrix for the element, referred to the preferred axes, are obtained by applying the transformation operator described above for both the  $+\theta$  and the  $-\theta$  orientations. The two resulting stiffness matrices are summed component-wise, and the components are then averaged, i.e. divided by two. This final stiffness matrix is then

given as input to all elements making up the physical layer with fibre orientation angle  $\pm\theta$ . By merging, or averaging, the stiffness values a new material is, in fact, introduced, where no fibre direction is defined. This is also considered as the most physically relevant approach. However, from introducing a new material it actually does not make sense to transform or express the stiffness properties, stresses or other quantities related to any of the two original  $+\theta$  or  $-\theta$  fibre orientations, for example in the post-processing part of the analysis. Nevertheless, “fibre stresses” obtained from the merged element stiffness cases are still included in this study and compared with the other approaches.

In the case of using *non-merged stiffness values*, the element stiffness matrices obtained by using the transformation operator for the  $+\theta$  and the  $-\theta$  orientations, are applied separately without any modifications. In this case, however, the four elements in the thickness direction that are making up the physical layer are given different stiffness properties. Two of the element layers are assumed to have a  $+\theta$  orientation of the fibres, while the  $-\theta$  orientation is adapted for the remaining two layers of the elements. From using this approach, we preserve the fibre direction, and may later relate stresses or other quantities to the real fibre coordinate system.

### 3.3.2 Composite elements

#### 3.3.2.1 Orientation of the thickness direction and element preferred axes

The definition of the thickness direction is important when applying composite elements. The thickness direction ( $e_2$ ) is shown in Figure 3.2, and is the second axis of the additional element coordinate system defined for composite elements. The direction of the first axis ( $e_1$ ) of this additional element coordinate system is oriented normal to the thickness direction, and is denoted the material direction. The third axis ( $e_3$ ) of the additional coordinate system is defined from using the right-hand rule.

The preferred axes for the composite elements are obtained from rotating an angle  $\theta$  about the thickness direction axis. Hence, in this case the first preferred axis is congruent with the local fibre direction. Note that the third preferred axis in this case is defined in the fibre plane, and that the second preferred axis is directed normal to the (fibre) plane. Also note that the positive fibre rotation angle for the composite elements corresponds to the negative rotation angle for the continuum elements, see Section 3.3.1.1. This is taken into account when defining the material properties and comparing the different approaches in the test cases presented here.

#### 3.3.2.2 Stiffness calculation

When applying the composite elements in MSC.Marc/Mentat, the material stiffness properties are given as input to Mentat by defining a reference material with orthotropic material properties. Additional input parameters are required for defining the rotation angle, and hence the orientation of the preferred axes, as well as the thickness of each internal element layer. For stability of the element, a minimum of two internal layers are required. Note that different input commands are employed in MSC.Marc/Mentat 2008r1 compared to later versions of the software.

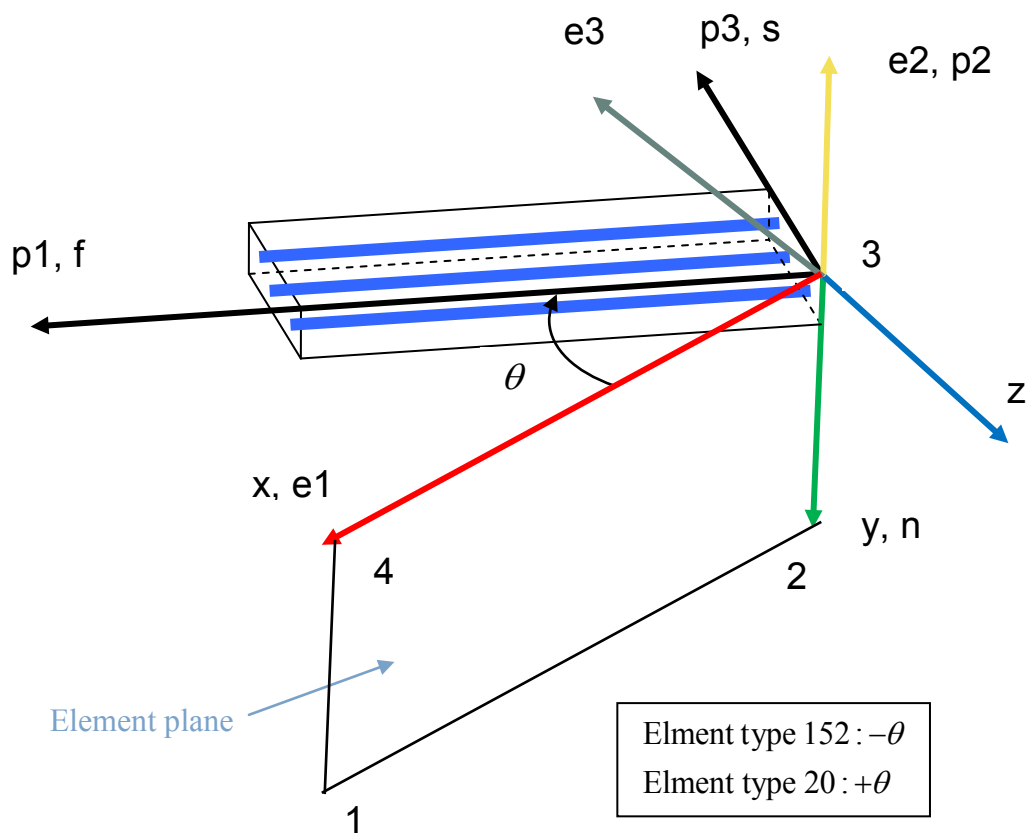


Figure 3.2 Axes  $(x,y,z)$ : Preferred element axes for the element, given by the ORIENTATIONS functionality in MSC.Marc/Mentat. Axes  $(e1,e2,e3)$ : Additional element axes for composite elements, where  $e1$  is the so-called material direction,  $e2$  is the thickness direction, and  $e3$  is defined by the cross product of  $e1$  and  $e2$ . Axes  $(p1,p2,p3)$ : Preferred element axes for the composite element, obtained from rotation an angle  $\theta$  about  $e2$ . Axes  $(f, s, n)$ : Fibre axes used for the continuum elements. Points 1,2,3,4: element node numbers. The same colours are applied in the figure as applied in Mentat.

As for the continuum elements is Section 3.3.1.2, two different approaches are applied in defining the stiffness properties:

- Merged stiffness values
- Non-merged stiffness values

In all cases, four internal plies are defined within each element. In the case of using *merged stiffness values* for the helical layers, two internal plies are given a positive fibre orientation and two plies a given negative fibre orientation. This should be close to merging the material properties for the entire element, as was done for the continuum elements; see Section 3.3.1.2. All elements making up the physical layer are then given the same properties. In case of using *non-*

*merged element stiffness values*, all internal plies are given the same fibre orientation. The composite elements making up the physical layer, representing the  $+\theta$  and  $-\theta$  orientation, are in this case given different properties, in the same way as for the continuum element non-merged stiffness properties approach.

### 3.4 Boundary conditions

Using the FEM, we must make sure that rigid body motions are avoided. In addition, symmetry boundary conditions must be applied at the symmetry plane at the right end; the length of the physical cylinder is 20 mm, whereas the length of the finite element geometric model is 10 mm. The same displacement boundary conditions are applied for both the continuum and composite element cases. Boundary conditions due to the applied loads will be described in Section 3.5.

The displacement boundary conditions for the axisymmetric model are shown in Figure 3.3. At the symmetry plane, the nodes are restricted from movement in the axial (global  $x$ ) direction. As part of the axisymmetric formulation the nodes are also restricted from movement in the circumferential (global  $z$ ) direction. Hence, the nodes on this edge are only allowed to move in the radial (global  $y$ ) direction.

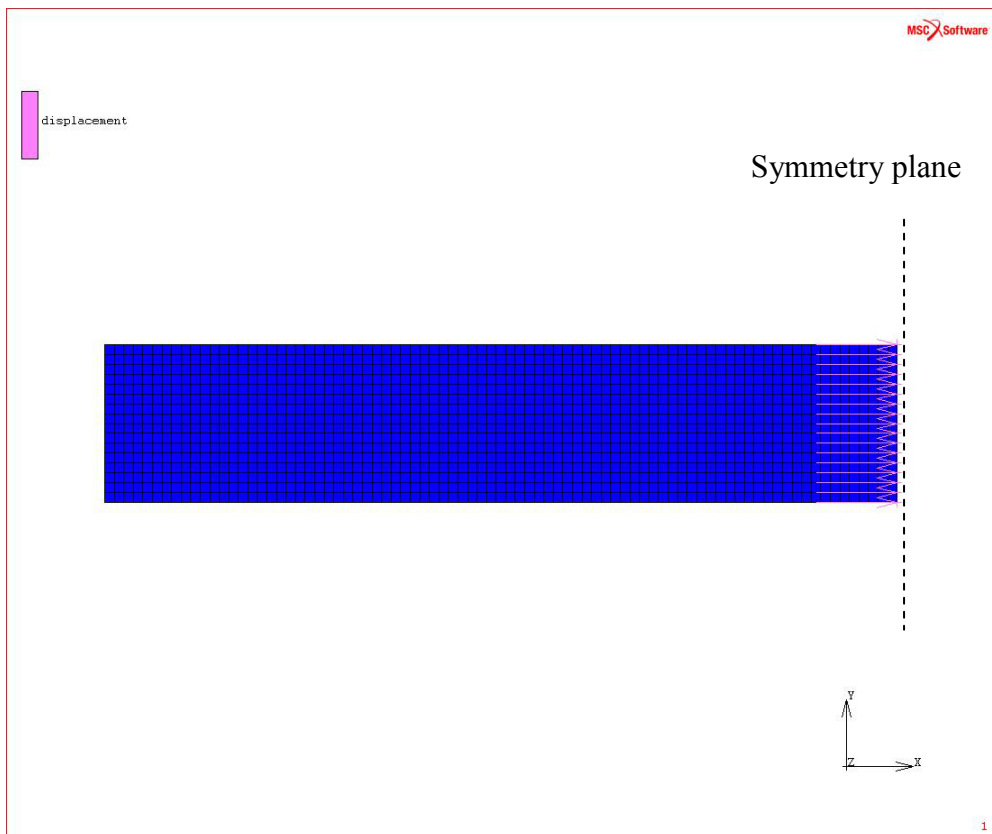


Figure 3.3 Displacement boundary conditions.

### 3.5 Applied loads

Two different cases are run:

- Open cylinder
- Closed cylinder

This requires different loads to be defined.

#### 3.5.1 Open cylinder

For the open cylinder case, an inner pressure  $p = 10$  MPa is applied as shown in Figure 3.4.

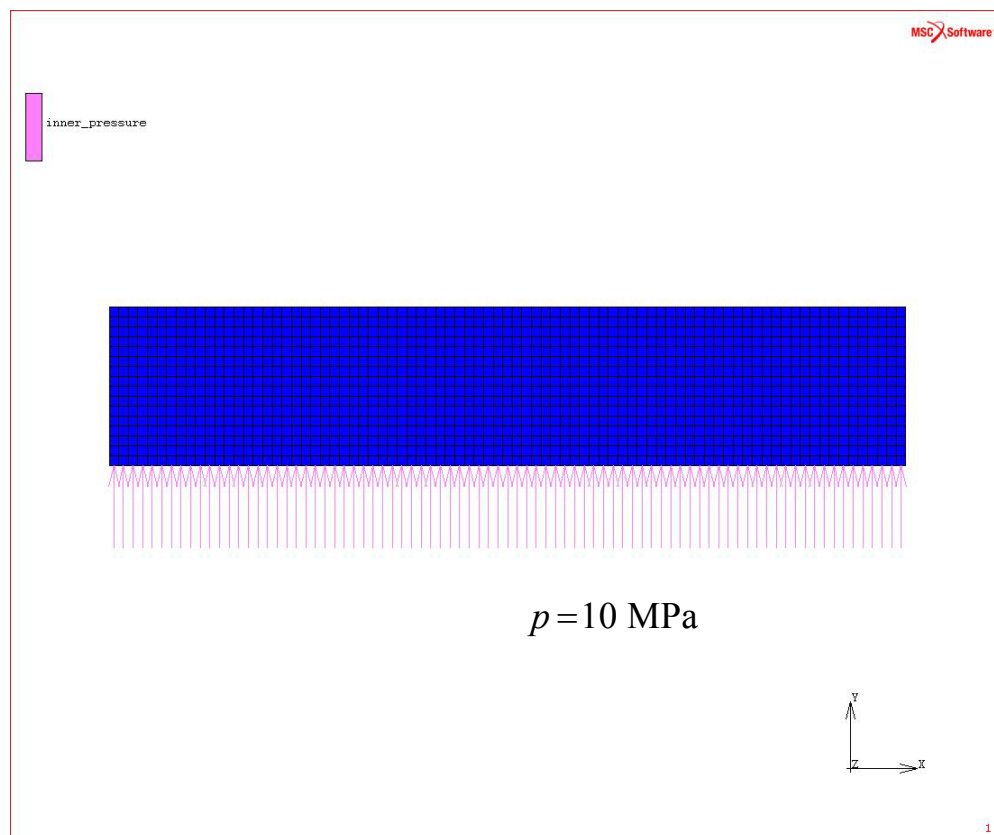


Figure 3.4 Applied loads, open cylinder.

#### 3.5.2 Closed cylinder

For the closed cylinder test case, the same pressure load is applied as for the open cylinder, see Section 3.5.1. In addition, to model an end cover at the left hand side of the finite element model, an additional load is applied, as shown in Figure 3.5.

The cover pressure is modelled in the form of a point load at the innermost node on left hand side of the cylinder, and yields,

$$F = Ap = \pi r^2 p \quad (3.1)$$

which for an inner pressure of  $p = 10$  MPa and an inner radius of  $r = 200$  mm , becomes  $F = 200 \times 200 \times 10 \times \pi = 1.257 \times 10^6$  N . Moreover, the nodes along the left hand side are linked to the innermost node, so that all nodes get the same displacement.

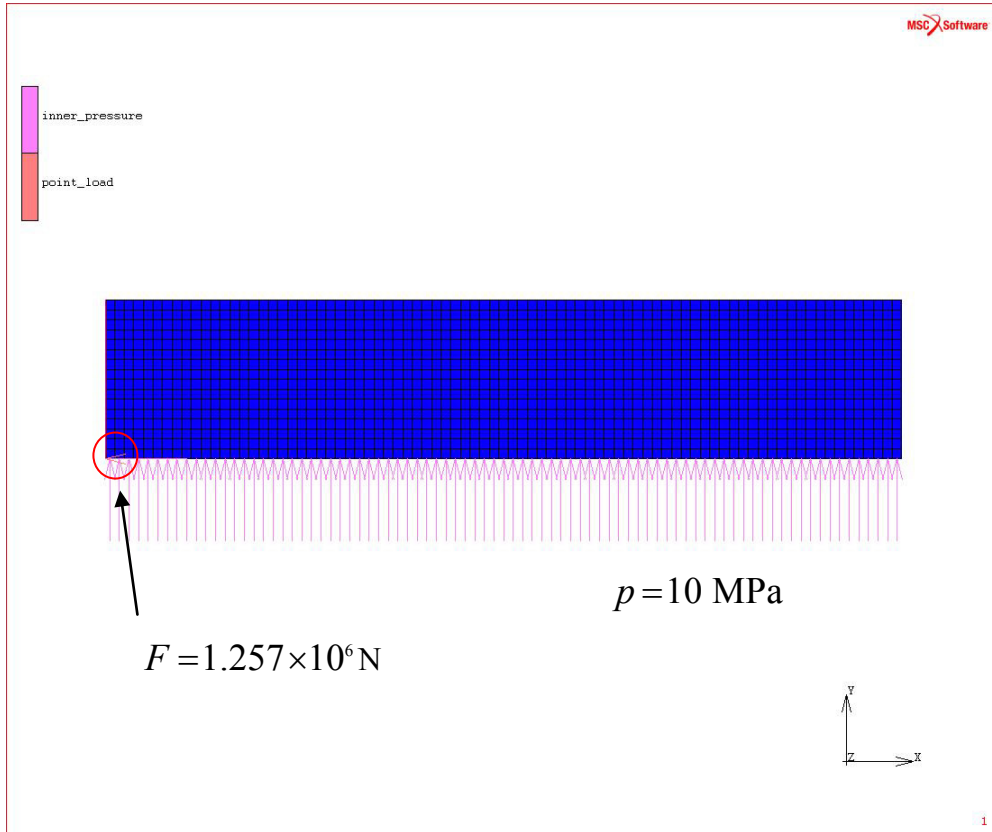


Figure 3.5 Applied loads, closed cylinder.

## 4 Analytical method

As mentioned in Section 3.1, the geometry of the cylinder is defined, so that it is possible to compare the numerical results with analytical expressions for a thin-walled composite cylinder. As a consequence of the large radius compared to the thickness, the curvature of the cylinder is small. Hence, the cylinder case can be modelled as a flat plate, with uni-axial or bi-axial loading, for the open and closed cylinder cases, respectively.

From general composite laminate theory, the stress-strain relation for each layer of the composite can be expressed as,

$$\begin{pmatrix} \sigma_{11} \\ \sigma_{22} \\ \sigma_{12} \end{pmatrix} = \begin{pmatrix} \bar{Q}_{11} & \bar{Q}_{12} & \bar{Q}_{16} \\ \bar{Q}_{12} & \bar{Q}_{22} & \bar{Q}_{26} \\ \bar{Q}_{16} & \bar{Q}_{26} & \bar{Q}_{66} \end{pmatrix} \begin{pmatrix} \varepsilon_{11} \\ \varepsilon_{22} \\ \varepsilon_{12} \end{pmatrix} \quad (4.1)$$

where the components of the above matrix are defined by,



$$\begin{aligned}
\bar{Q}_{11} &= Q_{11} \cos^4 \theta + Q_{22} \sin^4 \theta + 2(Q_{12} + 2Q_{66}) \cos^2 \theta \sin^2 \theta \\
\bar{Q}_{22} &= Q_{11} \sin^4 \theta + Q_{22} \cos^4 \theta + 2(Q_{12} + 2Q_{66}) \cos^2 \theta \sin^2 \theta \\
\bar{Q}_{12} &= (Q_{11} + Q_{22} - 4Q_{66}) \cos^2 \theta \sin^2 \theta + Q_{12} (\cos^4 \theta + \sin^4 \theta) \\
\bar{Q}_{66} &= (Q_{11} + Q_{22} - 2Q_{12} - 2Q_{66}) \cos^2 \theta \sin^2 \theta + Q_{66} (\cos^4 \theta + \sin^4 \theta) \\
\bar{Q}_{16} &= (Q_{11} - Q_{12} - 2Q_{66}) \cos^3 \theta \sin \theta - (Q_{22} - Q_{12} - 2Q_{66}) \cos \theta \sin^3 \theta \\
\bar{Q}_{26} &= (Q_{11} - Q_{12} - 2Q_{66}) \cos \theta \sin^3 \theta - (Q_{22} - Q_{12} - 2Q_{66}) \cos^3 \theta \sin \theta
\end{aligned} \tag{4.2}$$

where  $\theta$  is the rotation of the layer with respect to global axes, and

$$\begin{aligned}
Q_{11} &= \frac{E_L}{1 - \nu_{LT}\nu_{TL}} \\
Q_{22} &= \frac{E_T}{1 - \nu_{LT}\nu_{TL}} \\
Q_{12} &= \frac{\nu_{LT}E_T}{1 - \nu_{LT}\nu_{TL}} = \frac{\nu_{TL}E_L}{1 - \nu_{LT}\nu_{TL}} \\
Q_{66} &= G_{LT}
\end{aligned} \tag{4.3}$$

where  $E_L$  and  $E_T$  are the Young's moduli in the fibre direction and normal to the fibre direction, respectively,  $G_{LT}$  is the in-plane shear modulus, whereas  $\nu_{LT}$  and  $\nu_{TL}$  are the major and minor Poisson's ratio, respectively.

The total stiffness of the entire laminate is obtained from summing up the contribution from all plies,

$$\begin{pmatrix} N_{11} \\ N_{22} \\ N_{12} \end{pmatrix} = \begin{pmatrix} A_{11} & A_{12} & A_{16} \\ A_{12} & A_{22} & A_{26} \\ A_{16} & A_{26} & A_{66} \end{pmatrix} \begin{pmatrix} \varepsilon_{11} \\ \varepsilon_{22} \\ \varepsilon_{12} \end{pmatrix} \tag{4.4}$$

with

$$A_{ij} = \sum_{k=1}^n (\bar{Q}_{ij})_k (h_k - h_{k-1}), \quad n = \text{number of plies} \tag{4.5}$$

denoted the extensional stiffness matrix.

Our main concern is the in-plane deformation of a flat plate subjected to in-plane forces. Thus, the contribution from the plate curvature is not included in the above calculations. Moreover, no coupling stiffness matrix or bending stiffness matrix is defined for the interaction between the resultant forces and moments in the more general  $2 \times 2$  block matrix system that can be defined [3].

A simulator has been implemented in the commercial software package Diffpack [4] for calculating the in-plane stresses for each ply, as well as the global displacements. The code lines (.cpp file) for running the simulator are found in Appendix B.

## 5 Laminated Tube

Laminated Tube is an Excel-based application developed in an earlier project at FFI, based on general laminate theory [5] and applied for quick calculations of in-plane stresses in all plies of a cylindrically shaped composite structure subjected to loading. This tool is first of all employed in the first stage of the development of a new filament-wound structure, to get an estimate of the requirements for the thickness and lay-up. In the following, a short user's guide to Laminated Tube is provided.

### *Running the application on your local computer*

If copying the application to your computer, or moving it to a new folder on your computer, make sure that the drive and location (i.e. the path) is changed accordingly.

### *Geometry*

The geometry of the cylinder is defined by the inner radius.

### *Lay-up*

The composite lay-up is defined by the list of layers; layer orientation, layer thickness and material number.

### *Material properties*

The material parameters are given in a separate sheet called "MATERIALS". The material number in this sheet corresponds to the material number in the lay-up definition.

### *Open or closed tube*

It is possible to run both an open cylinder, or tube, case, as well as a partly or fully closed cylinder case. Tick off the "Closed tube" option in case of a closed cylinder test case.

### *Loads*

Different load cases are available: internal pressure, external pressure and torch. Note that the axial force, in case of a closed tube, is calculated automatically when ticking off the "Closed tube" option. Make sure that the axial load is manually set to zero (again) if an open cylinder case is run. Otherwise, the axial load is applied to the open cylinder.

### *Calculation*

The number of integration points is given by input. Calculations are run by pressing the "Run program" button.

### *Stress results*

The in-plane stresses, both referred to global axes and local fibre axes, are calculated, where  $x$  and  $y$  refer to the global axes for the laminate, whereas 1 and 2 refer to the local fibre axes. Stress values are calculated for all integration points, and are found in a separate sheet called “STRESS RESULTS”.

### *Plots*

Plots of the in-plane stress variation through the thickness are given on separate sheets.

### *Additional documentation*

No additional documentation for the use of the tool has been written. Together with the above short description, the user interface should be self-explanatory and sufficient for using the program in the current study.

## **6 Test cases**

Three test cases, or lay-ups, are run. For each lay-up, different simulations are performed for comparison of the above mentioned methodologies for calculating the element stiffness properties and the type of element. The FEA are compared with the analytical model results and the results from Laminated Tube.

Global displacements and in-plane stresses for each physical layer are reported in each case. The axial displacement is set to a positive value in case of elongation of the cylinder, and set to a negative value in case of contraction of the cylinder. The radial displacement is defined as positive for an increase in the cylinder radius. For the continuum element merged stiffness cases, the stress values refer to the direction of the material for a set of axes that are rotated an angle  $+\theta$ , i.e. corresponding to the fibre axes for the original  $+\theta$  layer. For the continuum element non-merged stiffness cases, the fibre coordinate axes are defined, and reported referred to the fibre axes. For the composite element cases, the element preferred axes are congruent with the fibre axes, and hence no transformation is needed in the post-processing part of the analysis.

For each case the results from the finite element analysis is listed together with the results from the analytical model and Laminated Tube. Note that for the analytical model and for Laminated Tube, non-merged stiffness properties are applied, i.e. separate layers for the  $+\theta$  and the  $-\theta$  fibre orientations are employed, independent of the methodology used in the corresponding finite element analysis.

### **6.1 Case #1: [45/90/45/90]**

This case is known to be a challenging case to model, and is seen as one of the “extreme” test cases for layered composite structures, when applying an axisymmetric model. Hence, it is a good case for testing the different modelling approaches and element types in MSC.Marc/Mentat.

The lay-up for this case is shown in Figure 6.1. The results from the simulations are shown in the following subsections.

90	0.5 mm
±45	0.5 mm
90	0.5 mm
±45	0.5 mm

Figure 6.1 Case #1. Lay-up.

### 6.1.1 Continuum elements

#### 6.1.1.1 Merged stiffness values – open cylinder

Table 6.1 [±45 / 90 / ±45 / 90], open cylinder. In-plane stresses (in MPa).

Orientation	Marc model			Analytical model			Laminated tube		
	$\sigma_{11}$	$\sigma_{22}$	$\sigma_{12}$	$\sigma_{11}$	$\sigma_{22}$	$\sigma_{12}$	$\sigma_{11}$	$\sigma_{22}$	$\sigma_{12}$
±45	72	72	61	194	12	59	200	8	59
90	1844	-46	0	1848	-44	0	1840	-46	0
±45	127	127	57	194	12	59	196	10	59
90	1838	-35	0	1848	-44	0	1830	-44	0

Table 6.2 [±45 / 90 / ±45 / 90], open cylinder. Displacements (in mm).

Marc model		Analytical model		Laminated tube	
Axial	Radial	Axial	Radial	Axial	Radial
-0.096	2.19	-0.087	2.21	-	-

#### 6.1.1.2 Variant #1: Non-merged stiffness values – open cylinder

Table 6.3 [+45 / +45 / -45 / -45 / 90]<sub>2</sub>, open cylinder. In-plane stresses (in MPa).

Orientation	Marc model			Analytical model			Laminated tube		
	$\sigma_{11}$	$\sigma_{22}$	$\sigma_{12}$	$\sigma_{11}$	$\sigma_{22}$	$\sigma_{12}$	$\sigma_{11}$	$\sigma_{22}$	$\sigma_{12}$
±45	138	5	61	194	12	59	200	8	59
90	1845	-46	0	1848	-44	0	1840	-46	0
±45	241	13	57	194	12	59	196	10	59
90	1839	-35	0	1848	-44	0	1830	-44	0

Table 6.4  $[+45/+45/-45/-45/90]_2$ , open cylinder. Displacements (in mm).

Marc model		Analytical model		Laminated tube	
Axial	Radial	Axial	Radial	Axial	Radial
-0.095	2.19	-0.087	2.21	-	-

#### 6.1.1.3 Variant #2: Non-merged stiffness values – open cylinder

Table 6.5  $[+45/-45/-45/+45/90]_2$ , open cylinder. In-plane stresses (in MPa).

Orientation	Marc model			Analytical model			Laminated tube		
	$\sigma_{11}$	$\sigma_{22}$	$\sigma_{12}$	$\sigma_{11}$	$\sigma_{22}$	$\sigma_{12}$	$\sigma_{11}$	$\sigma_{22}$	$\sigma_{12}$
$\pm 45$	144	5	61	194	12	59	200	8	59
90	1844	-46	0	1848	-44	0	1840	-46	0
$\pm 45$	240	12	57	194	12	59	196	10	59
90	1838	-34	0	1848	-44	0	1830	-44	0

Table 6.6  $[+45/-45/-45/+45/90]_2$ , open cylinder. Displacements (in mm).

Marc model		Analytical model		Laminated tube	
Axial	Radial	Axial	Radial	Axial	Radial
-0.095	2.19	-0.087	2.21	-	-

#### 6.1.1.4 Merged stiffness values – closed cylinder

Table 6.7  $[\pm 45/90/\pm 45/90]$ , closed cylinder. In-plane stresses (in MPa).

Orientation	Marc model			Analytical model			Laminated tube		
	$\sigma_{11}$	$\sigma_{22}$	$\sigma_{12}$	$\sigma_{11}$	$\sigma_{22}$	$\sigma_{12}$	$\sigma_{11}$	$\sigma_{22}$	$\sigma_{12}$
$\pm 45$	859	859	15	1645	99	17	1640	96	17
90	1186	110	0	1155	116	0	1160	112	0
$\pm 45$	857	857	15	1645	99	17	1630	97	17
90	1175	112	0	1155	116	0	1150	114	0

Table 6.8  $[\pm 45/90/\pm 45/90]$ , closed cylinder. Displacements (in mm).

Marc model		Analytical model		Laminated tube	
Axial	Radial	Axial	Radial	Axial	Radial
0.12	1.37	0.12	1.33	-	-

### 6.1.1.5 Variant#1: Non-merged stiffness values – closed cylinder

Table 6.9  $[+45 / +45 / -45 / -45 / 90]_2$ , closed cylinder. In-plane stresses (in MPa).

Orientation	Marc model			Analytical model			Laminated tube		
	$\sigma_{11}$	$\sigma_{22}$	$\sigma_{12}$	$\sigma_{11}$	$\sigma_{22}$	$\sigma_{12}$	$\sigma_{11}$	$\sigma_{22}$	$\sigma_{12}$
$\pm 45$	1618	94	15	1645	99	17	1640	96	17
90	1199	110	0	1155	116	0	1160	112	0
$\pm 45$	1624	96	15	1645	99	17	1630	97	17
90	1188	112	0	1155	116	0	1150	114	0

Table 6.10  $[+45 / +45 / -45 / -45 / 90]_2$ , closed cylinder. Displacements (in mm).

Marc model		Analytical model		Laminated tube	
Axial	Radial	Axial	Radial	Axial	Radial
0.13	1.38	0.12	1.33	-	-

### 6.1.1.6 Variant#2: Non-merged stiffness values – closed cylinder

Table 6.11  $[+45 / -45 / -45 / +45 / 90]_2$ , closed cylinder. In-plane stresses (in MPa).

Orientation	Marc model			Analytical model			Laminated tube		
	$\sigma_{11}$	$\sigma_{22}$	$\sigma_{12}$	$\sigma_{11}$	$\sigma_{22}$	$\sigma_{12}$	$\sigma_{11}$	$\sigma_{22}$	$\sigma_{12}$
$\pm 45$	1621	94	15	1645	99	17	1640	96	17
90	1191	110	0	1155	116	0	1160	112	0
$\pm 45$	1621	96	16	1645	99	17	1630	97	17
90	1180	112	0	1155	116	0	1150	114	0

Table 6.12  $[+45 / -45 / -45 / +45 / 90]_2$ , closed cylinder. Displacements (in mm).

Marc model		Analytical model		Laminated tube	
Axial	Radial	Axial	Radial	Axial	Radial
0.12	1.37	0.12	1.33	-	-

## 6.1.2 Composite elements

### 6.1.2.1 Merged stiffness values – open cylinder

The case is run with the non-positive definite option “on”.

Table 6.13  $[\pm 45 / 90 / \pm 45 / 90]$ , open cylinder. In-plane stresses (in MPa).

Orientation	Marc model			Analytical model			Laminated tube		
	$\sigma_{11}$	$\sigma_{33}$	$\sigma_{31}$	$\sigma_{11}$	$\sigma_{22}$	$\sigma_{12}$	$\sigma_{11}$	$\sigma_{22}$	$\sigma_{12}$
$\pm 45$	24	22	0	194	12	59	200	8	59
90	2004	-58	0	1848	-44	0	1840	-46	0
$\pm 45$	71	66	0	194	12	59	196	10	59
90	1972	-26	0	1848	-44	0	1830	-44	0

Table 6.14  $[\pm 45 / 90 / \pm 45 / 90]$ , open cylinder. Displacements (in mm).

Marc model		Analytical model		Laminated tube	
Axial	Radial	Axial	Radial	Axial	Radial
-0.12	2.41	-0.087	2.21	-	-

### 6.1.2.2 Non-merged stiffness values – open cylinder

The test case is run with the non-positive definite option “on”.

Table 6.15  $[+45 / +45 / -45 / -45 / 90]_2$ , open cylinder. In-plane stresses (in MPa).

Orientation	Marc model			Analytical model			Laminated tube		
	$\sigma_{11}$	$\sigma_{33}$	$\sigma_{31}$	$\sigma_{11}$	$\sigma_{22}$	$\sigma_{12}$	$\sigma_{11}$	$\sigma_{22}$	$\sigma_{12}$
$\pm 45$	26	24	0	194	12	59	200	8	59
90	2004	-57	0	1848	-44	0	1840	-46	0
$\pm 45$	70	65	0	194	12	59	196	10	59
90	1970	-26	0	1848	-44	0	1830	-44	0

Table 6.16  $[+45 / +45 / -45 / -45 / 90]_2$ , open cylinder. Displacements (in mm).

Marc model		Analytical model		Laminated tube	
Axial	Radial	Axial	Radial	Axial	Radial
-0.12	2.41	-0.087	2.21	-	-

### 6.1.2.3 Merged stiffness values – closed cylinder

The test case is run with the non-positive definite option “on”.

Table 6.17  $[\pm 45 / 90 / \pm 45 / 90]$ , closed cylinder. In-plane stresses (in MPa).

Orientation	Marc model			Analytical model			Laminated tube		
	$\sigma_{11}$	$\sigma_{22}$	$\sigma_{12}$	$\sigma_{11}$	$\sigma_{22}$	$\sigma_{12}$	$\sigma_{11}$	$\sigma_{22}$	$\sigma_{12}$
$\pm 45$	909	857	0	1645	99	17	1640	96	17
90	1152	115	0	1155	116	0	1160	112	0
$\pm 45$	907	855	0	1645	99	17	1630	97	17
90	1141	117	0	1155	116	0	1150	114	0

Table 6.18  $[\pm 45 / 90 / \pm 45 / 90]$ , closed cylinder. Displacements (in mm).

Marc model		Analytical model		Laminated tube	
Axial	Radial	Axial	Radial	Axial	Radial
0.13	1.33	0.12	1.33	-	-

#### 6.1.2.4 Non-merged stiffness values – closed cylinder

The test case is run with the non-positive definite option “on”.

Table 6.19  $[+45 / +45 / -45 / -45 / 90]_2$ , closed cylinder. In-plane stresses (in MPa).

Orientation	Marc model			Analytical model			Laminated tube		
	$\sigma_{11}$	$\sigma_{33}$	$\sigma_{31}$	$\sigma_{11}$	$\sigma_{22}$	$\sigma_{12}$	$\sigma_{11}$	$\sigma_{22}$	$\sigma_{12}$
$\pm 45$	909	856	0	1645	99	17	1640	96	17
90	1153	115	0	1155	116	0	1160	112	0
$\pm 45$	907	855	0	1645	99	17	1630	97	17
90	1142	117	0	1155	116	0	1150	114	0

Table 6.20  $[+45 / +45 / -45 / -45 / 90]_2$ , closed cylinder. Displacements (in mm).

Marc model		Analytical model		Laminated tube	
Axial	Radial	Axial	Radial	Axial	Radial
0.13	1.33	0.12	1.33	-	-

#### 6.1.3 Discussion

One first observation is that the stress values calculated using the analytical model and Laminated Tube are in accordance with each other. This verifies that both tools calculate in-plane stresses correctly. No simplifications for, or any assumptions about, a thin-walled cylinder are made in the implementation of Laminated Tube. Hence, it should also be applicable to composite cylinders with a lower thickness-to-radius ratio. In the following we therefore compare the FEM results with the analytical model, but implicitly also with Laminated Tube. Displacements are, however, only available for the analytical model.



Employing the continuum element type for the open cylinder test runs, we observe that the axial and radial displacements are the same when using merged and non-merged element stiffness values. The displacement values are also in accordance with the analytical calculations. Moreover, the two different non-merged variants, i.e. the cases with different stacking sequence of the +45 and -45 layers, do not seem to significantly alter the overall deformation of the structure. For the in-plane stresses, we observe that all the hoop layer values predicted by the FEA are in accordance with the analytical results. However, this is not the case for the helical layers, where, in particular, the normal stress values differ. When applying merged element stiffness values, the two in-plane normal stresses become equal. This is as expected from the material definition, but is far from what is obtained when using the analytical model, where each plus and minus fibre orientation is defined separately. Thus, using a merged element stiffness representation is not an appropriate approach if in-plane normal stresses for each physical layer are required. For the non-merged element stiffness value cases, the normal stresses for the helical layers are more in accordance with the analytical values. Note that a difference is obtained for the inner and outer helical layers, where the stresses in the innermost helical layer become too low, whereas the stresses in the outer helical layer become too high. For the shear stresses the values are in accordance with analytical results.

Applying composite elements for the open cylinder test runs, we observe that the axial displacement, in particular, becomes too high compared to the analytical calculations. The displacement values are the same for the merged and non-merged element stiffness representation. As for the continuum element cases, the normal stresses in the hoop layers are almost in accordance with the analytical calculations, but significantly higher. For the helical layers, the stress values differ considerably. Moreover, for the composite elements, the in-plane shear stress is zero in all layers, which is not correct for the helical layers.

Employing continuum elements for the closed cylinder test runs, we observe that the axial displacement is in accordance with analytical results. The radial displacement is a bit too large, but very close to the analytical value. In the same way as for the open cylinder case, the merged element stiffness approach results in normal stress values that are in accordance with analytical values for the hoop layers, though a bit higher. For the helical layers the two in-plane normal stress values become equal, and are not in accordance with the analytical values. On the other hand, for the non-merged element stiffness approach, the in-plane normal stresses in all physical layers are in accordance with the analytical results. The in-plane shear stresses are in accordance with the analytical values for all test runs.

Applying the composite elements for the closed cylinder test runs, the displacements are found to be in accordance with the analytical calculations both when employing merged element stiffness values and non-merged element stiffness values. The normal stresses in the hoop layers are in accordance with analytical values in both approaches. This is, however, not the case for the helical layers, where the two in-plane normal stresses are almost equal in value. This is what we also observe for the merged stiffness approach employing continuum elements. As for the open

cylinder cases, the in-plane shear stress becomes zero in all layers, which is not correct for the helical layers.

## 6.2 Case #2: [0/90/0/90]

This case is known to be one of the least challenging test cases when modelling a layered composite structure using an axisymmetric model. Hence, this case is also essential to examine for the different approaches and element types. Due to the layer orientation, only one test run is required for each combination of stiffness calculation approach and element type.

The physical layers of the test case are shown in Figure 6.2. The test run results are shown in the following subsections.

90	0.5 mm
0	0.5 mm
90	0.5 mm
0	0.5 mm

Figure 6.2: Case #2. Lay-up.

### 6.2.1 Continuum elements – open cylinder

Table 6.21  $[0/90]_2$ , open cylinder. In-plane stresses (in MPa).

Orientation	Marc model			Analytical model			Laminated tube		
	$\sigma_{11}$	$\sigma_{22}$	$\sigma_{12}$	$\sigma_{11}$	$\sigma_{22}$	$\sigma_{12}$	$\sigma_{11}$	$\sigma_{22}$	$\sigma_{12}$
0	0	86	0	-25	90	0	-24	86	0
90	1915	22	0	1920	25	0	1920	22	0
0	-42	87	0	-25	90	0	-22	88	0
90	1902	22	0	1920	25	0	1910	24	0

Table 6.22  $[0/90]_2$ , open cylinder. Displacements (in mm).

Marc model		Analytical model		Laminated tube	
Axial	Radial	Axial	Radial	Axial	Radial
-0.009	2.26	-0.003	2.26	-	-

### 6.2.2 Continuum elements – closed cylinder

Table 6.23  $[0/90]_2$ , closed cylinder. In-plane stresses (in MPa).

Orientation	Marc model			Analytical model			Laminated tube		
	$\sigma_{11}$	$\sigma_{22}$	$\sigma_{12}$	$\sigma_{11}$	$\sigma_{22}$	$\sigma_{12}$	$\sigma_{11}$	$\sigma_{22}$	$\sigma_{12}$
0	923	99	0	936	102	0	928	98	0
90	1917	66	0	1908	70	0	1910	66	0
0	925	100	0	936	102	0	930	100	0
90	1902	68	0	1908	70	0	1890	68	0

Table 6.24  $[0/90]_2$ , closed cylinder. Displacements (in mm).

Marc model		Analytical model		Laminated tube	
Axial	Radial	Axial	Radial	Axial	Radial
0.053	2.24	0.053	2.23	-	-

### 6.2.3 Composite elements – open cylinder

The test is run with the non-positive definite option “off”. Turning the option “on” does, however, not change the results.

Table 6.25  $[0/90]_2$ , open cylinder. In-plane stresses (in MPa).

Orientation	Marc model			Analytical model			Laminated tube		
	$\sigma_{11}$	$\sigma_{33}$	$\sigma_{31}$	$\sigma_{11}$	$\sigma_{22}$	$\sigma_{12}$	$\sigma_{11}$	$\sigma_{22}$	$\sigma_{12}$
0	4	89	0	-25	90	0	-24	86	0
90	1954	-2	0	1920	25	0	1920	22	0
0	1	90	0	-25	90	0	-22	88	0
90	1948	-2	0	1920	25	0	1910	24	0

Table 6.26  $[0/90]_2$ , open cylinder. Displacements (in mm).

Marc model		Analytical model		Laminated tube	
Axial	Radial	Axial	Radial	Axial	Radial
-0.03	2.33	-0.003	2.26	-	-

### 6.2.4 Composite elements – closed cylinder

The test is run with the non-positive definite option “on”.

Table 6.27  $[0/90]_2$ , closed cylinder. In-plane stresses (in MPa).

Orientation	Marc model			Analytical model			Laminated tube		
	$\sigma_{11}$	$\sigma_{33}$	$\sigma_{31}$	$\sigma_{11}$	$\sigma_{22}$	$\sigma_{12}$	$\sigma_{11}$	$\sigma_{22}$	$\sigma_{12}$
0	924	100	0	936	102	0	928	98	0
90	1944	67	0	1908	70	0	1910	66	0
0	926	101	0	936	102	0	930	100	0
90	1929	69	0	1908	70	0	1890	68	0

Table 6.28  $[0/90]_2$ , closed cylinder. Displacements (in mm).

Marc model		Analytical model		Laminated tube	
Axial	Radial	Axial	Radial	Axial	Radial
0.053	2.29	0.053	2.23	-	-

### 6.2.5 Discussion

In the same way as for the first test case, the analytical model and Laminated Tube calculate the same in-plane stress values. The analytical model results are employed in the following comparison with the FEA.

Employing continuum elements for the open cylinder test run, the axial displacement is found to be larger than the analytical value. The radial displacement is, however, in accordance with the analytical value. For the in-plane stresses, all values are in accordance with the analytical results, except for the normal stress in the fibre direction of the helical layers. The largest difference is found in the innermost helical layer.

Applying composite elements for the open cylinder test run, we observe that both the axial and radial displacement become larger than the analytical results. Moreover, the in-plane stress values are in accordance with the analytical results, except for the normal fibre stress in the helical layers and for the normal stress perpendicular to the fibre direction of the hoop layers. The in-plane shear stress is calculated correctly in this particular case.

Using continuum elements for the closed cylinder test run, one observes that both the displacements and the in-plane stresses are in accordance with analytical values.

Employing composite elements for the closed cylinder test run, one finds that the radial displacement becomes a bit too large, but the in-plane stresses are in accordance with the analytical results.

### 6.3 Case #3: $[10/90/30/90]$

This third test case represents a more realistic lay-up, which may be relevant for a real pressure vessel or a rocket motor case. The fibre orientation in the innermost and outermost helical layer differs in this case. The stacking of the element layers does not seem to affect the overall

deformation or the stresses, see Section 6.1. Thus, only one variant of the combination of using continuum elements and non-merged stiffness properties are included.

The lay-up is shown in Figure 6.3, and the simulation test results are shown in the following subsections.

90	0.5 mm
±30	0.5 mm
90	0.5 mm
±10	0.5 mm

Figure 6.3 Case #3. Lay-up.

### 6.3.1 Continuum elements

#### 6.3.1.1 Merged stiffness values – open cylinder

Table 6.29  $[\pm 10 / 90 / \pm 30 / 90]$ , open cylinder. In-plane stresses (in MPa).

Orientation	Marc model			Analytical model			Laminated tube		
	$\sigma_{11}$	$\sigma_{22}$	$\sigma_{12}$	$\sigma_{11}$	$\sigma_{22}$	$\sigma_{12}$	$\sigma_{11}$	$\sigma_{22}$	$\sigma_{12}$
±10	-80 – +60	81	17	-215	83	13	-213	80	13
90	1882	8	0	1898	12	0	1900	10	0
±30	49	79	26	264	67	34	265	65	34
90	1864	-11	0	1898	12	0	1890	11	0

Table 6.30  $[\pm 10 / 90 / \pm 30 / 90]$ , open cylinder. Displacements (in mm).

Marc model		Analytical model		Laminated tube	
Axial	Radial	Axial	Radial	Axial	Radial
-0.052	2.34	-0.018	2.24	-	-

### 6.3.1.2 Non-merged stiffness values – open cylinder

Table 6.31  $[+10/-10/90/+30/-30/90]$ , open cylinder. In-plane stresses (in MPa).

Orientation	Marc model			Analytical model			Laminated tube		
	$\sigma_{11}$	$\sigma_{22}$	$\sigma_{12}$	$\sigma_{11}$	$\sigma_{22}$	$\sigma_{12}$	$\sigma_{11}$	$\sigma_{22}$	$\sigma_{12}$
$\pm 10$	-67 – +58	82	12	-215	83	13	-213	80	13
90	1882	8	2	1898	12	0	1900	10	0
$\pm 30$	64	59	36	264	67	34	265	65	34
90	1864	-13	2	1898	12	0	1890	11	0

Table 6.32  $[+10/-10/90/+30/-30/90]$ , open cylinder. Displacements (in mm).

Marc model		Analytical model		Laminated tube	
Axial	Radial	Axial	Radial	Axial	Radial
-0.053	2.35	-0.018	2.24	-	-

### 6.3.1.3 Merged stiffness values – closed cylinder

Table 6.33  $[\pm 10/90/\pm 30/90]$ , closed cylinder. In-plane stresses (in MPa).

Orientation	Marc model			Analytical model			Laminated tube		
	$\sigma_{11}$	$\sigma_{22}$	$\sigma_{12}$	$\sigma_{11}$	$\sigma_{22}$	$\sigma_{12}$	$\sigma_{11}$	$\sigma_{22}$	$\sigma_{12}$
$\pm 10$	935	146	144	1005	95	5	998	92	5
90	1772	66	0	1762	70	0	1760	67	0
$\pm 30$	757	497	224	1177	89	12	1170	87	12
90	1759	69	0	1762	70	0	1750	69	0

Table 6.34  $[\pm 10/90/\pm 30/90]$ , closed cylinder. Displacements (in mm).

Marc model		Analytical model		Laminated tube	
Axial	Radial	Axial	Radial	Axial	Radial
0.06	2.07	0.056	2.06	-	-

### 6.3.1.4 Non-merged stiffness values – closed cylinder

Table 6.35  $[+10/-10/90/+30/-30/90]$ , closed cylinder. In-plane stresses (in MPa).

Orientation	Marc model			Analytical model			Laminated tube		
	$\sigma_{11}$	$\sigma_{22}$	$\sigma_{12}$	$\sigma_{11}$	$\sigma_{22}$	$\sigma_{12}$	$\sigma_{11}$	$\sigma_{22}$	$\sigma_{12}$
$\pm 10$	1005	92	5	1005	95	5	998	92	5
90	1774	66	0	1762	70	0	1760	67	0
$\pm 30$	1152	87	13	1177	89	12	1170	87	12
90	1760	67	0	1762	70	0	1750	69	0

Table 6.36 [+10/-10/90/+30/-30/90], closed cylinder. In-plane stresses (in MPa).

Marc model		Analytical model		Laminated tube	
Axial	Radial	Axial	Radial	Axial	Radial
0.06	2.08	0.056	2.06	-	-

### 6.3.2 Composite elements

#### 6.3.2.1 Merged stiffness values – open cylinder

The test case is run with the non-positive definite option “on”.

Table 6.37 [ $\pm 10/90/\pm 30/90$ ], open cylinder. In-plane stresses (in MPa).

Orientation	Marc model			Analytical model			Laminated tube		
	$\sigma_{11}$	$\sigma_{33}$	$\sigma_{31}$	$\sigma_{11}$	$\sigma_{22}$	$\sigma_{12}$	$\sigma_{11}$	$\sigma_{22}$	$\sigma_{12}$
$\pm 10$	-2	42	0	-215	83	13	-213	80	13
90	2033	-4	0	1898	12	0	1900	10	0
$\pm 30$	4	9	0	264	67	34	265	65	34
90	1996	-3	0	1898	12	0	1890	11	0

Table 6.38 [ $\pm 10/90/\pm 30/90$ ], open cylinder. Displacements (in MPa).

Marc model		Analytical model		Laminated tube	
Axial	Radial	Axial	Radial	Axial	Radial
-0.05	2.42	-0.018	2.24	-	-

#### 6.3.2.2 Non-merged stiffness values – open cylinder

Table 6.39 [+10/-10/90/+30/-30/90], open cylinder. In-plane stresses (in MPa).

Orientation	Marc model			Analytical model			Laminated tube		
	$\sigma_{11}$	$\sigma_{33}$	$\sigma_{31}$	$\sigma_{11}$	$\sigma_{22}$	$\sigma_{12}$	$\sigma_{11}$	$\sigma_{22}$	$\sigma_{12}$
$\pm 10$	-10 - +7	43	0	-215	83	13	-213	80	13
90	2033	-5	0	1898	12	0	1900	10	0
$\pm 30$	4	9	0	264	67	34	265	65	34
90	1996	-3	0	1898	12	0	1890	11	0

Table 6.40 [+10/-10/90/+30/-30/90], open cylinder. Displacements (in mm).

Marc model		Analytical model		Laminated tube	
Axial	Radial	Axial	Radial	Axial	Radial
-0.05	2.42	-0.018	2.24	-	-

### 6.3.2.3 Merged stiffness values – closed cylinder

The test case is run with the non-positive definite option “on”.

Table 6.41  $[\pm 10/90/\pm 30/90]$ , closed cylinder. In-plane stresses (in MPa).

Orientation	Marc model			Analytical model			Laminated tube		
	$\sigma_{11}$	$\sigma_{33}$	$\sigma_{31}$	$\sigma_{11}$	$\sigma_{22}$	$\sigma_{12}$	$\sigma_{11}$	$\sigma_{22}$	$\sigma_{12}$
$\pm 10$	1025	586	0	1005	95	5	998	92	5
90	1351	88	0	1762	70	0	1760	67	0
$\pm 30$	820	753	0	1177	89	12	1170	87	12
90	1340	90	0	1762	70	0	1750	69	0

Table 6.42  $[\pm 10/90/\pm 30/90]$ , closed cylinder. Displacements (in MPa).

Marc model		Analytical model		Laminated tube	
Axial	Radial	Axial	Radial	Axial	Radial
0.09	1.58	0.056	2.06	-	-

### 6.3.2.4 Non-merged stiffness values – closed cylinder

Table 6.43  $[+10/-10/90/+30/-30/90]$ , closed cylinder. In-plane stresses (in MPa).

Orientation	Marc model			Analytical model			Laminated tube		
	$\sigma_{11}$	$\sigma_{33}$	$\sigma_{31}$	$\sigma_{11}$	$\sigma_{22}$	$\sigma_{12}$	$\sigma_{11}$	$\sigma_{22}$	$\sigma_{12}$
$\pm 10$	1025	586	0	1005	95	5	998	92	5
90	1351	88	0	1762	70	0	1760	67	0
$\pm 30$	820	753	0	1177	89	12	1170	87	12
90	1340	90	0	1762	70	0	1750	69	0

Table 6.44  $[+10/-10/90/+30/-30/90]$ , closed cylinder. Displacements (in mm).

Marc model		Analytical model		Laminated tube	
Axial	Radial	Axial	Radial	Axial	Radial
0.09	1.58	0.056	2.06	-	-

### 6.3.3 Discussion

As for the two previous test cases, the analytical model and Laminated Tube predict the same level of stresses. The FEA results are compared with the analytical model results in the following.

Employing the continuum elements for the open cylinder test run, one observes that the axial and radial displacements become larger than what is calculated by the analytical model. For the in-plane stresses the values are in accordance with the analytical values, except for the normal stress in the fibre direction for the helical layers and the normal stress value perpendicular to the fibre



direction in the outermost hoop layer. The normal stress value in the fibre direction of the helical layers varies over the physical layer thickness and differs from the analytical value. For the normal stress in the hoop layers, the absolute value of the normal stress is the same, but the sign is opposite. The same differences are in this case found for both the merged and non-merged stiffness cases.

Applying the composite elements for the open cylinder test run, one observes that the axial and radial displacements are larger than calculated by the analytical model. Moreover, the in-plane stresses in the helical layers are different from the analytical results. This is also the case for the normal stress perpendicular to the fibre direction for the hoop layers. The shear stress value is zero in all layers, which is incorrect for the helical layers.

Using continuum elements for the closed cylinder test runs, the axial and radial displacement are in accordance with the analytical results. For the merged element stiffness case, the normal stresses for the helical layers are different from analytical predictions, but for the hoop layers the normal stresses are in agreement with the analytical results. Thus, the main trend is similar to the observations for Case #1 in Section 6.1. For the non-merged stiffness approach, all normal stress values are in accordance with the analytical results. The in-plane shear stresses agree well with the analytical calculations for both approaches.

Using composite elements for the closed cylinder case, the axial and radial displacement become smaller compared to the analytical results. This is also the case for the normal stresses. The in-plane shear stress is again zero for all layers, and this is not correct for the helical layers.

## 7 Summary and conclusions

In this study, different tools are developed and applied for calculating the deformation and layer stresses for a thin-walled filament-wound composite cylinder. FEA are performed, including different approaches for calculating the stiffness properties for each physical layer and different element types. Both an open cylinder case and a closed cylinder case are run. The results from the FEA are compared with analytical results and Laminated Tube. Theory for a thin-walled pressure tank is applied for the analytical model.

One main conclusion from the study is that Laminated Tube calculates correct stress values. In all test cases, the values are in accordance with the analytical model results. No assumptions or simplifications for a thin-walled tube are made in the implementation. Hence, this tool should also be applied for other geometries and lay-ups, and is an important tool for quick estimation of the lay-up of a cylindrical shaped structure exposed to an inner pressure load.

For the FEA, it is first of all concluded that continuum axisymmetric elements may be used for calculating the overall deformation of a layered cylindrical structure. The FEA results are in accordance with the analytical model results and the results from Laminated Tube. Note, however, that special care should be taken for the open cylinder case. If only the global axial and

radial displacements are required, the merged element stiffness approach may be applied. If in-plane normal stresses for each layer of the structure are required in addition, the non-merged stiffness value approach must be employed. This latter conclusion is as expected, because by merging the stiffness values for different fibre orientations a new material is introduced, and the fibre direction is no longer defined.

The axisymmetric composite element type tested in this study is found not to be satisfactory. First of all, the in-plane shear stress becomes zero; the shear stress is only calculated correctly for the  $[0/90]_2$  case. Moreover, the deformations and in-plane normal stresses are not in accordance with analytical values. As a conclusion, composite element type 152 in MSC.Marc/Mentat 2008r1 should not be used for this kind of calculations. It should be remarked that the errors observed when using the composite element type may have been corrected in later versions of the software.

The results and the knowledge obtained from this study will be important in future development of new rocket motor cases and other filament-wound structures.

## **Acknowledgements**

The authors would like to thank Stein Tenden (Nammo) for useful discussions and input, and Bernt B. Johnsen for reading and giving useful comments to the final version of this report.

## Appendix A Material data

Table A1 Material properties for the composite referred to local fibre axes.

Material property (fibre in epoxy)	Unit	Value
Fiber volume		
$E_{11}$	MPa	170000
$E_{22}$	MPa	8000
$E_{33}$	MPa	8000
$G_{12}$	MPa	3000
$G_{23}$	MPa	2564
$G_{13}$	MPa	3000
$\nu_{12}$		0.3
$\nu_{13}$		0.3
$\nu_{23}$		0.4
$\nu_{21}$		0.0141
$\nu_{32}$		0.4
$\nu_{31}$		0.0141

## Appendix B Analytical model

The Diffpack code for running the uni-axial and bi-axial test cases is given below.

```
#include <ArraysSimple.h>

int main (int nargs, const char** args)
{
    // General initialization of the simulator
    initDiffpack (nargs, args);
    global_menu.init ("Stresses and deformations of thin-walled,
cylindrical structures made of composites", "Analysis of thin-
walled structures");

    // Specification of input parameters

    // We start by specifying the number of layers, the thickness
    // of each layer and the lay-up
    int no_layers;
    Vec(real) layer_thickness, layer_orientation;
    no_layers = 8;
    layer_thickness.redim (no_layers);
    layer_orientation.redim (no_layers);

    // Here we assume the thickness of all the (single) layers to
    // be 0.25 mm
    layer_thickness.fill (0.25);

    // Case I
    layer_orientation(1) = 90.0;
    layer_orientation(2) = 90.0;
    layer_orientation(3) = 45.0;
    layer_orientation(4) = -45.0;
    layer_orientation(5) = 90.0;
    layer_orientation(6) = 90.0;
    layer_orientation(7) = 45.0;
    layer_orientation(8) = -45.0;

    // Case II
    /*
    layer_orientation(1) = 90.0;
    layer_orientation(2) = 90.0;
    layer_orientation(3) = 0.0;
    layer_orientation(4) = 0.0;
```

```

layer_orientation(5) = 90.0;
layer_orientation(6) = 90.0;
layer_orientation(7) = 0.0;
layer_orientation(8) = 0.0;
*/

// Case III
/*
layer_orientation(1) = 90.0;
layer_orientation(2) = 90.0;
layer_orientation(3) = 30.0;
layer_orientation(4) = -30.0;
layer_orientation(5) = 90.0;
layer_orientation(6) = 90.0;
layer_orientation(7) = 10.0;
layer_orientation(8) = -10.0;
*/

// Specification of material input parameters required in the
// laminate analysis method adopted
real E_L, E_T, nu_LT, nu_TL, G_LT;

E_L = 170000.0; // MPa
E_T = 8000.0; // MPa
G_LT = 3000.0; // MPa
nu_LT = 0.3;
nu_TL = nu_LT*E_T/E_L;

// Specification of geometric parameters
real radius, length;
radius = 201.0; // mm
length = 10.0; // mm

// Specification of indicator for type of vessel/pipe
// Open pipe/vessel => vessel_indicator = 0.0
// Closed pipe/vessel => vessel_indicator = 1.0

real vessel_indicator;
// Open pipe/vessel
vessel_indicator = 0.0;

// Closed pipe/vessel
// vessel_indicator = 1.0;

```

```

// Specification of loading - inner pressure
real pressure;
pressure = 10.0;      // MPa

// Introduction of parameters and quantities that are needed
// in the analysis and can be calculated from the input
// parameters included above.

// Parameters for the stiffness properties of a layer
real Q_11, Q_22, Q_12, Q_66;
Q_11 = E_L/(1.0 - nu_LT*nu_TL);
Q_22 = E_T/(1.0 - nu_LT*nu_TL);
Q_12 = nu_TL*E_L/(1.0 - nu_LT*nu_TL);
Q_66 = G_LT;

// Q_loc - stiffness matrix for a lamina related to local fibre
// axes and engineering strains
// Q_loc_mod - stiffness matrix for a lamina related to local
// fibre axes and tensor strains - this one may easily be
// transformed to represent the lamina stiffness related to a
// set of global axes/arbitrary coordinate system

Mat(real) Q_loc, Q_loc_mod;
Q_loc.redim (3);
Q_loc.fill (0.0);
Q_loc_mod.redim (3);
Q_loc_mod.fill (0.0);

Q_loc(1,1) = Q_11;
Q_loc(1,2) = Q_12;
Q_loc(2,1) = Q_12;
Q_loc(2,2) = Q_22;
Q_loc(3,3) = Q_66;

Q_loc_mod = Q_loc;
Q_loc_mod(3,3) = 2.0*Q_66;

// Declaration of variables/parameters needed in the
// program/analysis
int i;
real phi;           // orientation of current layer
real total_thickness; // total thickness - to be updated

```

```

total_thickness = 0.0;          // initialization

// Stiffness matrices for a lamina related to a set of
// global (or arbitrary) axes.

// Q_glob - stiffness matrix for a lamina related to
// engineering strains
// Q_glob_mod - stiffness matrix for a lamina related to tensor
// strains,

Mat(real) Q_glob, Q_glob_mod;
Q_glob.redim (3);
Q_glob.fill (0.0);
Q_glob_mod.redim (3);
Q_glob_mod.fill (0.0);

// Transformation tensors - for the transition between fibre
// axes and global axes.
Mat(real) T, T_inv;
T.redim (3);
T_inv.redim (3);

// Stiffness matrix for the entire laminate.
// Only the A matrix from the laminate theory presented in
// Agarwal and Broutman is included in the present analysis.

Mat(real) A_mat, A_mat_inv;
A_mat.redim (3);      A_mat.fill (0.0);
A_mat_inv.redim (3);  A_mat_inv.fill (0.0);

// Vectors containing the load per unit width and the in-plane
// strains are declared here.

Vec(real) N_vec, eps_vec;
N_vec.redim (3);      N_vec.fill (0.0);
eps_vec.redim (3);    eps_vec.fill (0.0);

// Matrix needed in some preliminary calculations

Mat(real) help;
help.redim(3);

```

```

// Loop over all the layers in order to calculate the
// laminate stiffness matrix A_mat.

for (i=1; i<=no_layers; i++) {

    total_thickness += layer_thickness(i);

    // M_PI = 3.14159265....
    phi = 2.0*M_PI*layer_orientation(i)/360.0;
    Q_glob.fill (0.0);
    Q_glob_mod.fill (0.0);
    help.fill (0.0);

    T(1,1) = sqr(cos(phi));
    T(1,2) = sqr(sin(phi));
    T(1,3) = 2.0*sin(phi)*cos(phi);
    T(2,1) = sqr(sin(phi));
    T(2,2) = sqr(cos(phi));
    T(2,3) = -2.0*sin(phi)*cos(phi);
    T(3,1) = -sin(phi)*cos(phi);
    T(3,2) = sin(phi)*cos(phi);
    T(3,3) = sqr(cos(phi)) - sqr(sin(phi));

    T.inverse (T_inv);
    help.prod (T_inv, Q_loc_mod);
    Q_glob_mod.prod (help, T);
    Q_glob = Q_glob_mod;
    Q_glob(1,3) = 0.5*Q_glob_mod(1,3);
    Q_glob(2,3) = 0.5*Q_glob_mod(2,3);
    Q_glob(3,3) = 0.5*Q_glob_mod(3,3);

    Q_glob.mult (layer_thickness(i));
    A_mat.add (Q_glob, 1.0);
}

// The loading of the laminate is determined through the
// inner pressure.

// sigma_x is only needed in case of a closed vessel/pipe.
// This is accounted for through the parameter
// 'vessel_indicator'

```



```

real sigma_x, sigma_y;

sigma_x = pressure*radius/(2.0*total_thickness);
sigma_y = pressure*radius/total_thickness;

// Actual loading (per unit width/length) for the laminate
N_vec(1) = vessel_indicator*sigma_x*total_thickness;
N_vec(2) = sigma_y*total_thickness;

// Solution procedure, i.e. calculation of in-plane strains
// with respect to the global set of axes

A_mat.inverse (A_mat_inv);
A_mat_inv.prod (N_vec, eps_vec);

// Dump statements for axial and radial displacements

s_o << "\n Axial displacement = " << eps_vec(1)*length << '\n';
s_o << "\n Radial displacement = " << eps_vec(2)*radius <<
'\n';

// We want to derive stress values with respect to the fiber
// axes for each lamina. At the moment, global engineering
// strains for the laminate have been obtained. The procedure
// is as follows:
// 1. Modify the global engineering strains to global tensor
// strains
// 2. Loop over the layers of the laminate - for each layer do
// 3. Transform global tensor strains to local (fiber) tensor
// strains
// 4. Modify local tensor strains to local engineering strains
// 5. Calculate (and dump) local (fiber) stresses (for each
// lamina)

Vec(real) eps_vec_mod, eps_vec_loc, eps_vec_loc_mod;
eps_vec_mod.redim (3);
eps_vec_mod.fill (0.0);
eps_vec_loc.redim (3);
eps_vec_loc.fill (0.0);
eps_vec_loc_mod.redim (3);
eps_vec_loc_mod.fill (0.0);

eps_vec_mod = eps_vec;

```

```

eps_vec_mod(3) = 0.5*eps_vec(3);

Vec(real) sigma_loc;
sigma_loc.redim (3);
sigma_loc.fill (0.0);

for (i=1; i<=no_layers; i++) {

    // M_PI = 3.14159265....
    phi = 2.0*M_PI*layer_orientation(i)/360.0;

    T(1,1) = sqr(cos(phi));
    T(1,2) = sqr(sin(phi));
    T(1,3) = 2.0*sin(phi)*cos(phi);

    T(2,1) = sqr(sin(phi));
    T(2,2) = sqr(cos(phi));
    T(2,3) = -2.0*sin(phi)*cos(phi);

    T(3,1) = -sin(phi)*cos(phi);
    T(3,2) = sin(phi)*cos(phi);
    T(3,3) = sqr(cos(phi)) - sqr(sin(phi));

    T.prod (eps_vec_mod, eps_vec_loc_mod);

    eps_vec_loc = eps_vec_loc_mod;
    eps_vec_loc(3) = 2.0*eps_vec_loc_mod(3);

    Q_loc.prod (eps_vec_loc, sigma_loc);

    sigma_loc.print (oform ("FILE=sigma_loc_layer_%d.dta", i));
}

return 0;
}

```

## Appendix C      Mentat input files

The Mentat module PyMentat is applied in generating input files for the test cases presented in this report. The input files are referred to as *Mentat input files* and are written in the Python language.

The following Mentat input files are applied:

- `cylinder_1.py`: Case #1. Continuum elements. Merged stiffness values. Open and closed cylinder.
- `cylinder_2.py`: Case #1. Continuum elements. Non-merged values, variant #1. Open and closed cylinder.
- `cylinder_3.py`: Case #1. Continuum elements. Non-merged values, variant #2. Open and closed cylinder.
- `cylinder_4.py`: Case #2. Continuum elements. Open and closed cylinder.
- `cylinder_5.py`: Case #3. Continuum elements. Merged stiffness values. Open and closed cylinder.
- `cylinder_6.py`: Case #3. Continuum elements. Non-merged values and closed cylinder.
- `comp_cylinder_1.py`: Case #1. Composite elements. Non-merged values. Open and closed cylinder.
- `comp_syylinder_2.py`: Case #2. Composite elements. Non-merged values. Open and closed cylinder.
- `comp_cylinder_3.py`: Case #3. Composite elements. Non-merged values. Open and closed cylinder.
- `comp_cylinder_4.py`: Case #1. Composite elements. Merged values. Open and closed cylinder.
- `comp_cylinder_5.py`: Case #3. Composite elements. Merged values. Open and closed cylinder.

## References

- [1] "MSC Software, [www.mscsoftware.com](http://www.mscsoftware.com)," 2011.
- [2] T. Thorvaldsen, "An introduction to numerical modeling of the front end of a rocket motor case," Forsvarets forskningsinstitut, FFI-rapport 2008/01787, 2008.
- [3] B. G. Agarwal, L. J. Broutman, and K. Chandrashekhara, *Analysis and performance of fiber composites*, 3rd ed John Wiley & Sons, Inc., 2006.
- [4] "Diffpack, [www.diffpack.com](http://www.diffpack.com)," 2011.
- [5] C. T. Herakovich, *Mechanics of fibrous composites* John Wiley & Sons, Inc., 1998.